Solvent Effect on the Electronic Spectra of Azine Dyes under Alkaline Condition

Soumen Basu,[†] Sudipa Panigrahi,[†] Snigdhamayee Praharaj,[†] Sujit Kumar Ghosh,[†] Surojit Pande,[†] Subhra Jana,[†] Anjali Pal,[‡] and Tarasankar Pal*[,†]

Department of Chemistry, Indian Institute of Technology, Kharagpur-721302, India, and Department of Civil Engineering, Indian Institute of Technology, Kharagpur-721302, India

Received: September 4, 2006; In Final Form: November 20, 2006

Thiazine dye, methylene blue (MB), oxazine dye, nile blue (NB), and phenazine-based dye, neutral red (NR), bear a similar basic dye skeleton with a distinctively different central heteroatom. All of them are extracted into nonpolar organic solvent from alkaline solution. The role of the heteroatom on the respective dye skeletons and redox potentials of the dyes has been examined to signature the stability of the species in organic solvent and the results have been substantiated through geometry optimization and wave function analysis at the density functional theory level. The effect of solvent polarity on the electronic absorption spectra of the three nonionic benzenoid species has been investigated with an intention to investigate the solvatochromic behavior of these compounds.

1. Introduction

Since the first decades of the 20th century, the chemistry of dyes has attracted much attention of the scientists from theoretical and experimental viewpoints.[1,2] The study of dyes, particularly the color−structure relationships, drew from structural and physical organic chemistry, including resonance theory, molecular orbital (MO) methods, and electronic spectra get tremendous momentum.[3,4] Later on, many research activities have been put forward in the literature concerning the effect of solvent polarity on the formation of adduct of different dyes. These investigations provide distinct information to account the effect of solvent polarity.[5−7] In this event, the solvent dependent properties are subjected to rigorous mathematical analysis, which rationalize solvent effects in terms of the properties of the medium.[8]

Ionic dye molecules in a solution might uptake counterions and form nonionic adducts which can play a significant role on the photophysical properties of these dyes in varied solvent systems. In some other case the molecule becomes nonionic by losing labile ions. In either case aromaticity becomes the general feature. Three nontoxic azine dyes, viz., methylene blue, nile blue, and neutral red have their perceptible biological importance. The change in color for the three dyes (MB, NB, and NR) in different medium is quite visible and clear. These dyes are also very much appreciated owing to their simple structure. Methylene blue (MB, 3,7-bis(dimethylamino)phenothiazin-5-ium chloride) is a basic, water-soluble, nontoxic, blue, cationic thiazine dye.[1,4] It is used as an oxidation−reduction indicator in chemistry and biology, as a sensitizer in photo-oxygenation, and as an electron exchanger with photogalvanic effect. It has several medicinal applications such a treating urinary tract infections, distinguishing between cancerous and normal tissue,[9] etc. As a secondary use, it is effective against various external protozoans, including ichthyophthirius, chilodonella, ichthyobodo (costia), and epistylis. On the other hand, neutral red (NR, 3-amino-7-dimethylamino-2-methyl phenazine) is a phenazine-based dye, which is widely used as a pH sensor and biological stain.[10−13] Because of the nontoxic nature of NR, the dye has been extensively used for staining cellular particles.[2,10] The dye is a good photodynamic photosensitizer,[13] and now it finds application as a probe for neuronal activity. Again, nile blue (5-amino-4-(diethylamino)benzo[*a*]-phenazoxonium hydrogen chloride) is a versatile, nontoxic visible phenoxazine dye with heterocyclic planar and rigid structure and with many applications in analytical chemistry, photoscience, materials science, and molecular biology.[3] Its planar hydrophobic phenoxazine moiety is expected to facilitate the intercalation of NB into the relatively nonplanar interior of the DNA helix.[14] Keeping the skeleton of the dye molecules in mind and considering all the above biological importance, we intend to look into the solvatochromic behavior of all the three dye molecules in a series of solvent systems.

All the three dye molecules, viz., MB, NB, and NR, possess a similar basic dye skeleton, but they bear distinctively different heteroatom of S, O, and N respectively. We have examined the electronic spectra of MB, NB, and NR and their nonionic entities in a series of solvents. The formation of these nonionic species has been rationalized from spectroscopic evidence. A comparative study has been made between the electronic spectra and stability of the three nonionic species in a sequence of solvents. Finally, the results have been substantiated through geometry optimization and frontier orbital analysis at the density functional theory level. The change in λ_{max} in different solvents has been explained in terms of solvent polarity on the electron-transfer process of all the three adducts.

2. Experimental

2.1. Reagents and Instruments. All the reagents used were of AR grade. Solvents for spectroscopic determinations were of spectroscopic grade, and all the solvents were dried before use. MB, NB, and NR were purchased from Aldrich and were used after repeated crystallization from alcohol. All the dye molecules contain Cl^- as the counterion. Sodium hydroxide

* To whom correspondence should be addressed. E-mail: tpal@chem.iitkgp.ernet.in.
† Department of Chemistry, Indian Institute of Technology.
‡ Department of Civil Engineering, Indian Institute of Technology.

10.1021/jp065740u CCC: $37.00
Published on Web 01/06/2007

(NaOH) was purchased from Merck. Double distilled water was used throughout the course of the investigation.

The absorption spectrum of each solution was recorded in a Spectrascan UV 2600 digital spectrophotometer (Chemito, India) in a 1-cm quartz cuvette, and the solvent background was subtracted each time. Electrospray ionization (ESI) mass spectra were taken using Waters LCT mass spectrometer. Raman spectra were obtained with a Renishaw Raman Microscope, equipped with a He−Ne laser excitation source emitting at a wavelength of 633 nm, and a Peltier cooled (−70 °C) charge-coupled device (CCD) camera. For an atomistic understanding of the structure−property relationship geometry optimization have been carried out at the well-accepted density functional level of B3LYP with a basis of 6-31G+(d, p) and theoretical calculations have been performed through the Gaussian 03 program suite.

2.2. Transformation of Ionic Dye into Nonionic Species. In a test tube, an aliquot of NR solution (0.1 mM) and NaOH (0.1 mM) were mixed, and the final volume of the solution was made to 3 mL. The mixture was shaken, and 3 mL of toluene was placed above the aqueous layer. The solution in the test tube was shaken well and allowed to equilibrate. After 1 h, the toluene layer was separated from the aqueous phase. An aliquot of 30 μL of the highly concentrated solution in toluene was diluted to 3 mL with a series of desired solvents (polar and nonpolar) so that final concentration of this nonionic species became 1 μM. The solvent effect was studied by measuring the changes in the absorption maximum of the solution using the spectrophotometer. The same procedure was followed for NB and MB.

3. Results and Discussion

Solvent effect is commonly used to describe a range of intermolecular interactions between solute molecules and the solvent in which they are dissolved. The organization of solvent molecules surrounding a solute molecule alters the ground and excited electronic and vibrational energy states of the solute. As a consequence of these perturbations, the nonradiative energy relaxation processes in a solute molecule is strongly affected by the solvent polarity. However, due to specific interactions between the solute and the solvent molecules, the intensity, shape, and absorption maxima in the electronic spectra of the solutes in solution also depend strongly on the nature of solvent.

Aqueous solution of NaOH does not show any characteristic absorption maximum in the range of 450−750 nm. On the other hand, MB, NB, and NR have strong absorption bands in the red region of the visible spectrum. Upon addition of an aqueous solution of NaOH (0.1 mM) to aqueous NR solution (0.1 mM), absorption maximum (λ_{max}) is blue-shifted to ~455 nm from the original peak position (λ_{max} ~ 528 nm). It was noted that neither NR nor NaOH could be extracted individually in toluene. But, when toluene was kept above the aqueous layer containing both NR and NaOH in a mixture and shaken well, the toluene layer turned yellow leaving the aqueous layer colorless. This is due to the formation of a nonionic, aromatic species out of NR and OH^- ion, and this species formation facilitates the swift movement of the species from aqueous layer to the organic phase.[15] Parts A, B, and C of Figure 1 show the extinction spectra of the MB, NB, and NR in water (trace a) and the corresponding non-ionic species in the aqueous (trace b) and organic phases (trace c), respectively. Insets in all the figures show the transfer of these nonionic species from aqueous to the organic solvents. Generally, the appearance of a shoulder at a shorter wavelength (trace a) in the optical spectra of aqueous solutions of these ionic dyes can be attributed to the aggregate formation. The splitting of the optical spectra is due to the excitonic coupling between transition dipoles on neighboring molecules. In other words, the dipole−dipole interaction between the adjacent molecules splits the electronic transitions into a broadband of states with different frequencies.

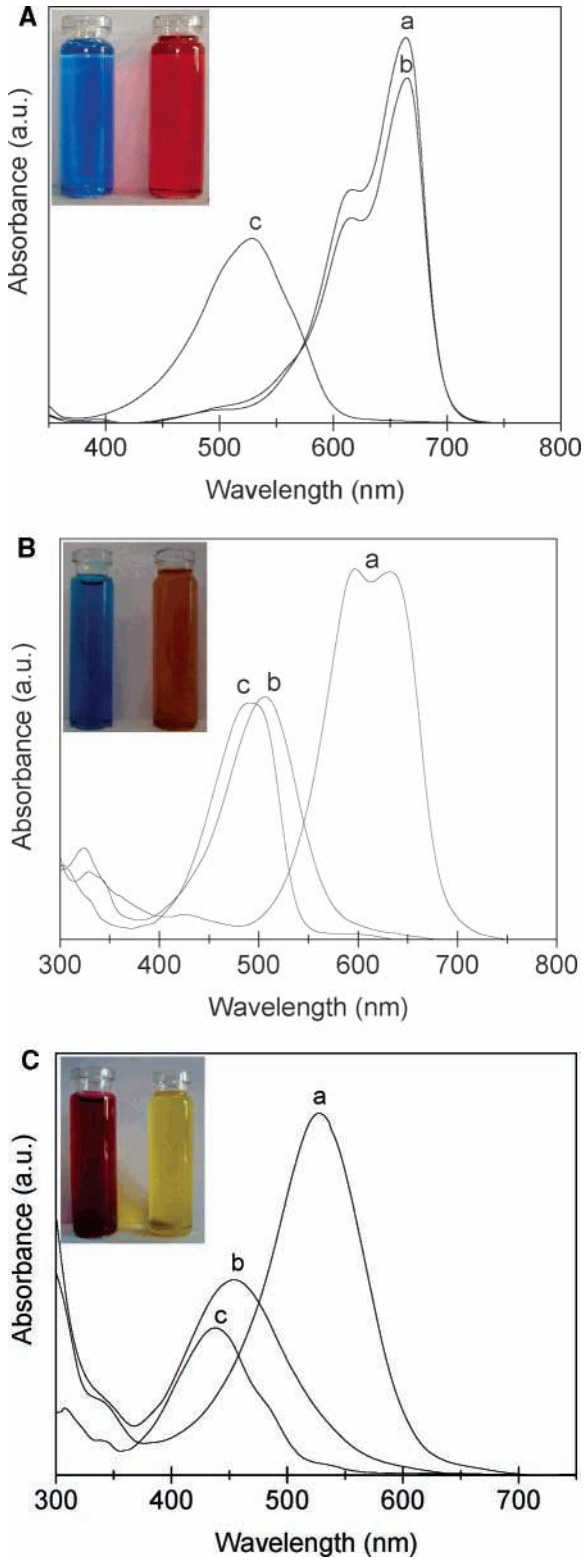

Figure 1. Absorption spectra of (A) MB, (B) NB, and (C) NR in which (a) aqueous solution of the dye, (b) nonionic benzenoid species in aqueous phase, and (c) nonionic benzenoid species in organic phase. Inset in all figures shows the extraction of the nonionic benzenoid species from aqueous to the organic phase.

SCHEME 1: Schematic Presentation of the Formation of Nonionic Benzenoid Species in Alkaline Condition and Regeneration of the Dye in Acidic Condition

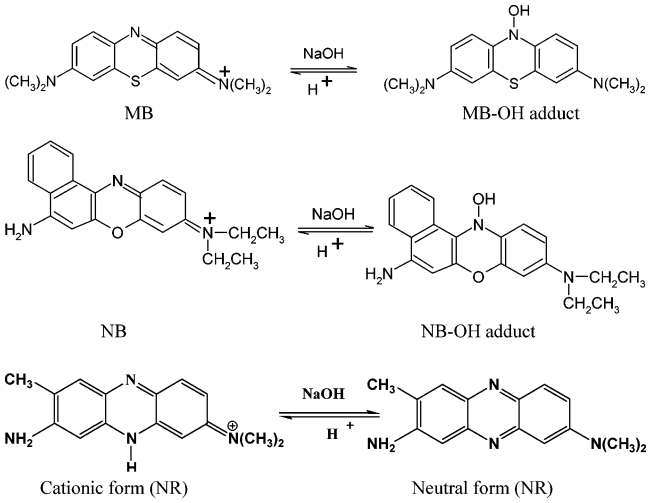

It is reported that the reduced form of the dye might be produced due to a nucleophilic attack upon the central nitrogen of the dye molecules by a good nucleophile, such as the thiolate anion of cysteine, cysteine sulfinate, cyanide, or the carbanion of vitamin B1.[16] Here, the attachment might be favored because this type of adduct formation would allow the two outer benzene rings to aromatize. In the present experiment, the nucleophile OH^- ion attacks the central nitrogen of MB and NB molecules but abstracts the H from NR. In all the three cases OH^- generates nonionic aromatic species from the parent dye molecules. This is because of the fact that the central nitrogen atom of all the three dyes is electron deficient. The color of the nonionic species turned red for MB, orange for NB, and yellow for NR in toluene. The red or orange or yellow colored solution immediately turned blue/red when spotted onto a silica-gel-coated thin-layer chromatography (TLC) plate. Even the mild acidic environment of silica gel destabilizes the benzenoid form and thus generates the respective but original water-soluble dye molecules on the TLC plates, suggesting that the dye−OH interaction/H abstraction is weak and reversible. Again, the stability of the benzenoid species in toluene/aqueous medium were tested by the addition of electrolytes, e.g., NaCl, KCl, Na_2SO_4, or dilute acid. Always reversal of quinonoid species was noted and colored organic layer becomes colorless and the aqueous (colorless) layer becomes blue/red. Explicitly, this is due to the dehydroxylation of the benzenoid moiety for MB and NB and protonation for NR case, which is illustrated in Scheme 1. Again, upon the addition of NaOH solution, the nonionic species are regenerated. No solid products are isolated from these studies. The counterions of the original dye molecules remain in the aqueous medium, and they do not interact with the nonionic, benzenoid species in organic medium.

The benzenoid form of NR in toluene when subjected to ESI mass analysis (cation mode), showed the molecular ion peak at *m*/*z* 253 in the highest mass region (see Supporting Information Figure 1). On the other hand, the quinonoid form of NR showed its molecular ion peak at *m*/*z* 254 in its ESI spectrum (cation mode) (see Supporting Information Figure 2). The benzenoid species (i.e., MB−OH and NB−OH) obtained from MB and NB were subjected to ESI mass analysis (cation mode), which confirmed that both the products are nonionic, N-hydroxylated benzenoid species of the corresponding parent molecules. The mass spectrum of the adduct evolved from MB showed the peak at *m*/*z* 301 in the highest mass region due to the molecular ion.

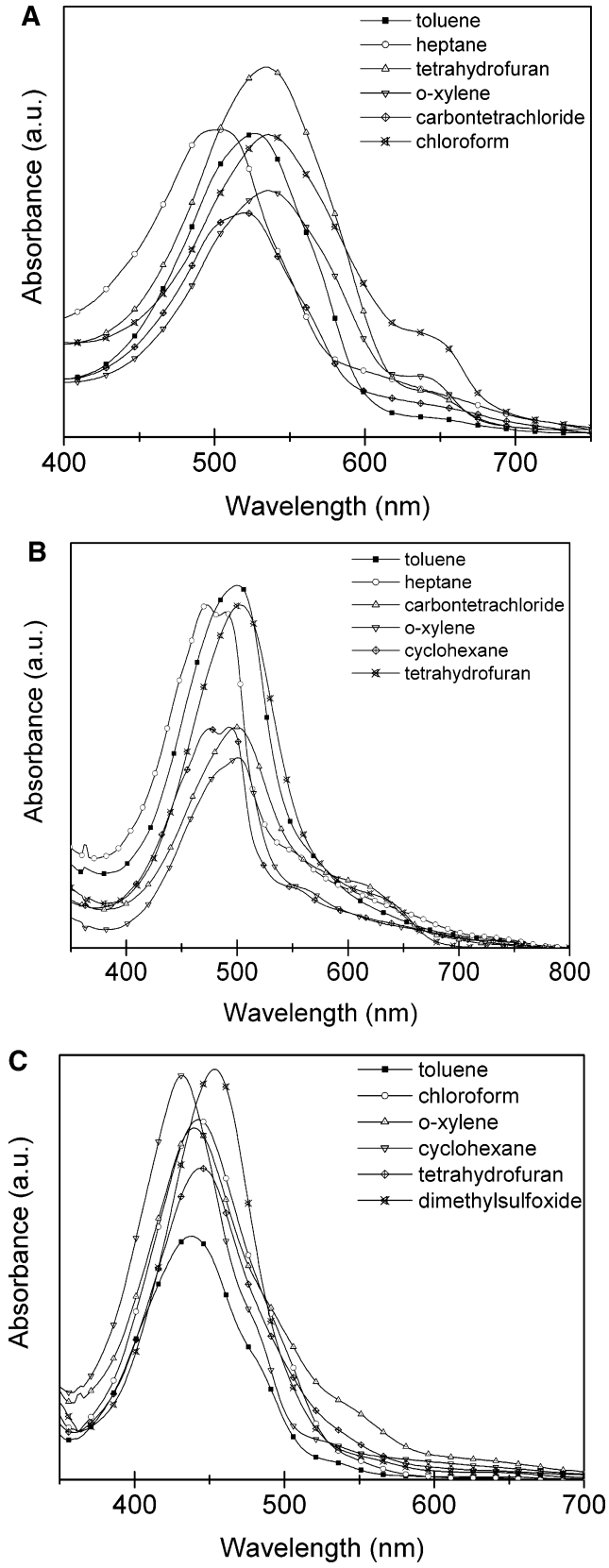

Figure 2. Absorption spectra of (A) MB−OH, (B) NB−OH, and (C) NR (neutral form) in a sequence of organic solvents.

This on subsequent fragmentation showed peak at *m*/*z* 270 ($M^{+\bullet}$−OH, −Me) and *m*/*z* 257 ($M^{+\bullet}-NMe_2$). The adduct of NB, on mass analysis, also showed its molecular ion peak at *m*/*z* 335. The molecular ion on further fragmentation showed peak at *m*/*z* 318 ($M^{+\bullet}$−OH). The mass spectra of both

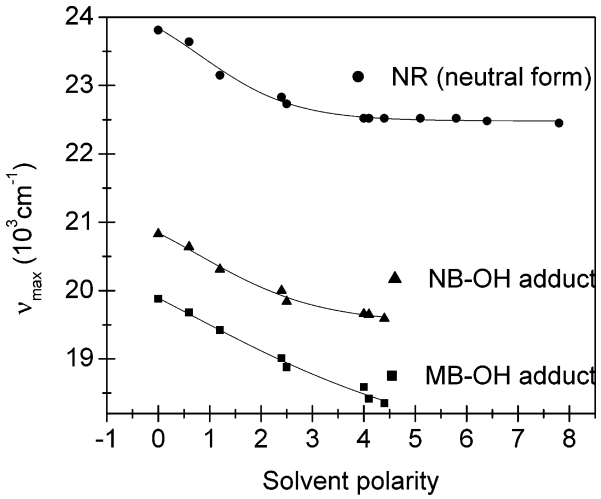

Figure 3. Plot of ν_{max} of the three nonionic benzenoid species in various solvents as a function of the solvent polarity of the medium.

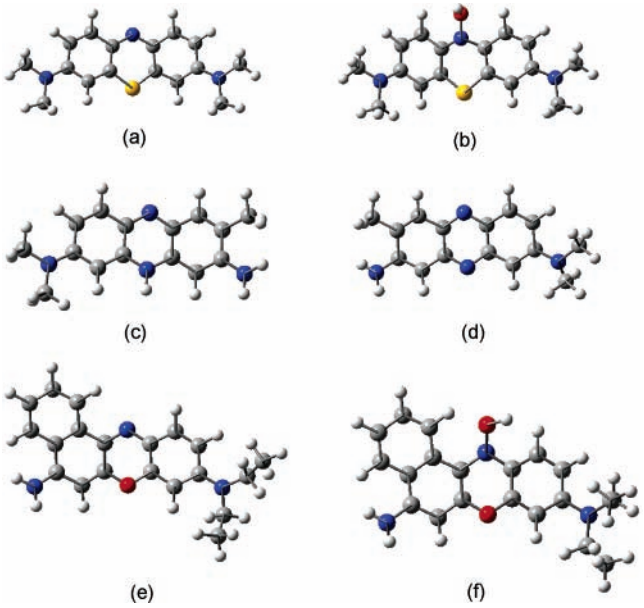

Figure 4. Ground state optimized structures of (a) MB, (b) MB−OH, (c) NR (cationic form), (d) NR (neutral form), (e) NB, and (f) NB−OH.

the products are included as Supporting Information (Figure 3 and Figure 4).

The benzenoid structure of NR (1) molecule was authenticated from ^{1}H NMR spectral analysis. The compound was isolated from the toluenic extract on evaporation under reduced pressure. The spectrum was run in a 400-MHz NMR instrument in d_6-DMSO solvent. The ^{1}H NMR spectrum of the structure (1) showed the aromatic methyl protons (ring C) appeared at δ 2.30 as a three-proton singlet. The methyl protons for the $-NMe_2$ group (ring A) appeared at δ 3.09 as a six-proton sharp singlet. The appearance of a two-proton singlet in the downfield region at δ 5.99 is due to the amino protons (ring C). All the aromatic protons appeared in separate regions. The two aromatic protons appearing as a singlet at δ 7.62 and δ 6.87 could be assigned to the protons present in the ortho and meta positions, respectively, to the aromatic $-CH_3$ group (ring C). The protons appearing in the most downfield region at δ 7.80 (1H, d, J = 8 Hz) are due to the proton meta to the $-NMe_2$ group (ring A). The other two protons in the same ring appeared at δ 7.46 (1H, dd, J_1 = 2.5 Hz, J_2 = 8 Hz) and δ 6.79 (1H, d, J = 2.5 Hz).

TABLE 1: Wavelength of the Absorption Maxima of the MB−OH, NB−OH, and NR (Neutral Form) in Different Organic Solvents

solvent	polarity[a]	λ_{max} of MB−OH adduct	λ_{max} of NB−OH adduct	λ_{max} of NR (neutral form)
heptane	0.0	503	480	420
cyclohexane	0.2	508	481	423
carbontetrachloride	1.6	515	496	432
toluene	2.4	526	500	438
o-xylene	2.5	534	504	440
tetrahydrofuran	4.0	535	506	444
chloroform	4.1	545	509	444
ethylacetate	4.4	547	510	444
acetone	5.1	b	b	443
acetonitrile	5.8	b	b	444
dimethylformamide	6.4	b	b	443
dimethylsulfoxide	7.2	b	b	450
water	9.0	662	513	455

[a] Polarity parameters by John A. Byers from Phenomenex catalog, 2003 http://www.Phenomenex.com. [b] Dehydroxylation.

On the basis of the foregoing ^{1}H NMR data, the compound was assigned the structure

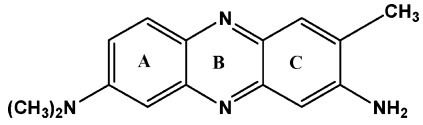

(1)

Because of the instability of both the adducts (MB−OH and NB−OH) in a polar environment the IR spectra in KBr matrix and characteristic NMR spectra in dry solvents could not be obtained to designate the presence of associated −OH functionality with the dye molecules. The adducts, i.e., the benzenoid structures, are very sensitive to the polar solvents, silica gel, and electrolytes. So the Raman measurements (laser light 633 nm with 2.5-mW laser power) were performed. Interestingly, both the adducts furnished sharp peaks at 2915 and 3060 cm^{-1} **(**see Supporting Information Figures 5 and 6**)**. There happens to be no signal at all in the 2500−3100-cm^{-1} region for the dye molecules. So, the signals unambiguously supported the adduct formation. Again, an increase in the polarity of the solvent system by HCl completely vanished the peaks regenerating quinonoid structures for the dye molecules.

For the real time monitoring of the electronic spectra of these benzenoid species due to changes in solvent polarity, the NaOH mediated aromatic species in the toluene layer were suspended in a sequence of polar and nonpolar solvents. In practice, an aliquot of 30 μL of the highly concentrated solution in toluene was diluted to 3 mL with the desired solvents so that final concentration of this benzenoid species became 1 μM. All the solutions thus contained ~1% of toluene so that the contribution of toluene to the changes in the extinction spectra can be neglected. Now, the normalized (i. e., solvent background was subtracted) spectra of all the solutions were measured. The positions of the absorption maxima, λ_{max} with the variation in solvent polarity for the three nonionic benzenoid species, are summarized in Table 1. It is seen that the absorption band shows a red shift on changing the solvent from low polarity to high polarity (solvent polarity from 0 to 9.0) that is shown in parts A, B, and C of Figure 2. The polar solvents with large dielectric constant behave as an ionic medium and are, therefore, considered effectively to stabilize the dyes in the excited state, which have more polar structures than the dyes in the ground

TABLE 2: Low-Frequency Vibrations for the Molecular Systems Considered in the Present Study (in cm^{-1})

	ω_1	ω_1	ω_1	ω_1	ω_1
MB	32.19	40.08	54.92	57.32	110.17
NB	23.93	32.88	57.06	66.22	74.77
NR neutral	41.49	42.64	72.98	85.84	107.27
MB−OH	19.29	20.09	28.32	61.88	73.04
NB−OH	17.86	27.25	43.94	56.72	67.06
NR cationic	39.14	45.21	67.84	102.55	133.18

state. Thus, the origin of the red shift observed for the dyes in polar solvent is due to the stabilization of the dyes in the excited state leading to the longer shifts of the absorption maxima of the dyes. It is known that the contribution of different forces such as dipole−dipole, dipole−induced dipole, and electrostatic forces are expected to contribute significantly in polar systems. Blanchardt[7] had shown that protic solvents associate significantly with an excited oxazine solute.

It is also seen that the absorption band shows only a moderate red shift on changing the solvent from low polarity to very high polarity for NR (420−455 nm), but for MB (503−662 nm) and NB (480−513 nm), it shows a dramatic red shift as the solvent polarity is increased. However, for all three aromatized species, λ_{max} shifts to the red in polar solvents. This is due to the stabilization of the excited state of the benzenoid species in polar solvents. The excited state of NR is less polar than the excited state of MB and NB. In case of MB, due to the high polarizability of sulfur the electron pair on the sulfur atom is more delocalized with the adjacent π-electrons. As a result, the H-bond/polar interaction between the N−OH and the solvent is more pronounced in case of MB. For NB, the higher electronegativity of oxygen makes the lone pair more localized, and hence it can directly participate in polar interaction with solvents. In case of NR, both these effects are minimum and therefore, we observe smaller red shift. So, the polar solvent stabilizes the excited state of MB and NB more than the excited-state of NR. As a consequence, a dramatic red shift of λ_{max} with polar solvent is observed for MB and NB. The change in intensity of the absorption spectra of the adduct relates to its difference in solubility in different solvent systems. A plot of absorption maxima, ν_{max} as a function of solvent polarity, is shown in Figure 3. Negative slopes of the curves indicate the shift of absorption maxima, ν_{max}, in all the three cases. Maximum shift was observed for MB, then NB and minimum shift was noted for NR case.

For an atomistic understanding of the structure−property relationship in our systems, we have performed geometry optimization for the ground states of MB, NB, NR, and their corresponding benzenoid structures at the well-accepted nonlocal density functional level of Becke's 3-parameter Lee−Yang−Parr functional (B3LYP) with a basis of 6-31G+(d,p).[17]

The geometry optimizations are performed without any symmetry constraints. All the calculations have been performed through the Gaussian 03 program suite.[18] The optimized structures are shown in Figure 4. We have performed additional frequency calculations to locate the minimal energy structures. In Table 2, we report the lowest five frequencies for all of our molecular systems. A clear inference from the optimization of the structures is that while for the dyes, the three rings remain planar, on aromatization the central ring becomes puckered for MB and NB molecules. The puckering angles for MB−OH and NB−OH are 8.5 and 2.9, respectively. Such puckering arises primarily due to steric interactions of the incoming −OH group with C−H groups of the aromatic rings on either side. Further calculations at the ZINDO/AM1 level shows that for the

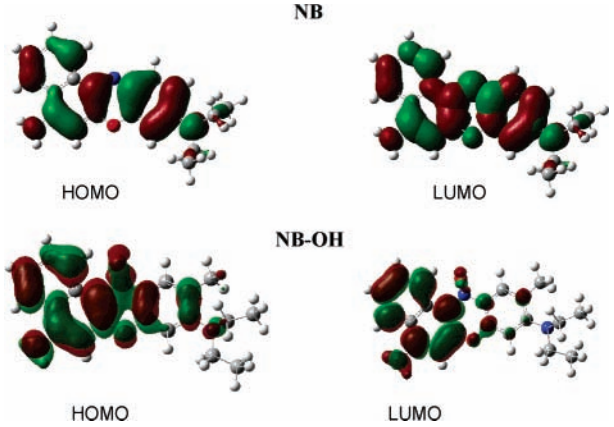

Figure 5. HOMO and LUMO plots for NB and NB−OH adduct.

compounds, the λ_{max} shifts to lower wavelengths (blue shift) upon hydroxylation and this compares fairly well with our experimental blue shifts. The maximum blue shift of 98 nm occurs for NB−OH in water. In Figure 5, we have plotted the highest occupied molecular orbitals (HOMO) and lowest unoccupied molecular orbitals (LUMO) for NB−OH. Clearly seen, that while for NB both the HOMO and the LUMO orbitals are substantially delocalized over the entire molecule, for NB−OH, the electrons in the frontier orbitals are localized on one ring. The observation remains same for NR case but this is a simple case of quinonoid to benzenoid structure change by H abstraction in alkaline condition.

Among the three benzenoid species of the dye molecules, MB−OH and NB−OH easily interact with polar solvents through direct charge-transfer interaction. This happens because of the facile removal of −OH group of the benzenoid species resulting in the reversible spectral shifts. On the contrary same polar solvent systems are incapable of the reversal of ionic form of NR. This relates to the higher stability of the nonpolar benzenoid form of NR in comparison to the other two species. Thus, we could perform the NMR analysis for NR case only. This might have a bearing with the standard electrode potential values of the dye molecules (MB_{ox}/MB_{red} = 1.08 V, NB_{ox}/NB_{red} = 1.4 V, and NR_{ox}/NR_{red} = −0.325 V vs NHE). From the electrode potential values, it is clear that among the three dyes, MB and NB are more favorable oxidants than NR in the experimental condition. Therefore, in polar solvents both MB and NB adducts reversibly generate dye molecules (quinonoid forms) displacing the −OH group but reversible protonation/deprotonation takes place in case of NR.

4. Conclusion

Azine dyes, MB and NB, form weak adducts with NaOH in the aqueous phase and the adducts can be extracted in an organic layer. On the other hand, OH^- abstracts H^+ for NR and makes the molecule fully aromatic. All of the three nonionic benzenoid species are unstable and acid sensitive, but the adducts of MB and NB are comparatively less stable than the species of NR. A red shift in the absorption maxima is observed with increasing solvent polarity. The absorption maximum shows only a moderate red shift on changing the solvent from low polarity to very high polarity for NR, but for MB and NB, it shows a dramatic red shift as the solvent polarity is increased. It may be further spelled out that the MB−OH adduct may be employed, because of its high sensitivity of λ_{max} shift in polar solvent, to investigate the solvent polarity taking the shift of λ_{max} into consideration. These results have been rationalized in the light of the distinct central

heteroatom in the dye skeleton and the geometry optimization at the density functional theory level.

Acknowledgment. We are thankful to the IIT, Kharagpur, CSIR & UGC, New Delhi for financial assistance and Dr. Ayan Datta for discussions.

Supporting Information Available: ESI mass spectra (cation mode) of NR (both neutral and cationic form), MB−OH, and NB−OH; Raman spectra of MB, MB−OH, NB, and NB−OH. This material is available free of charge via the Internet at http://pubs.acs.org.

References and Notes

(1) McRae, E. G.; Kasha, M. In *Physical Processes in Radiation Biology*; Augenstein, L., Mason, R., Rosenberg, B., Eds.; Academic Press: New York, 1964.

(2) (a) Valdes-Aguilera, O.; Neckers, D. C. *Acc. Chem. Res.* **1989**, *22*, 171−177. (b) Buncel, E.; Rajagopal, S. *Acc. Chem. Res.* **1990**, *23*, 226−231. (c) Reichardt, C. *Chem. Soc. Rev.* **1992**, *21*, 147−153.

(3) Huangxian, J.; Yongkang, Y.; Yonglin, Z. *Electrochim. Acta*. **2005**, *50*, 1361−1367.

(4) Ghosh, S. K.; Kundu, S.; Mandal, M.; Pal, T. *Langmuir* **2002**, *18*, 8756−8760.

(5) Blanchard, G. J.; Cihal, C. A. *J. Phys. Chem*. **1988**, *92*, 5950−5954.

(6) Kubinyi, M.; Grofcsik, A.; Papai, I.; Jones, W. *J. Chem. Phys.* **2003**, *286*, 81−96.

(7) Blanchard, G. J. *J. Phys. Chem*. **1991**, *95*, 5293−5299.

(8) Basu, S.; Ghosh, S. K.; Kundu, S.; Nath, S.; Panigrahi, S.; Praharaj, S.; Pal, T. *Chem. Phys. Lett*. **2005**, *407*, 493−497.

(9) Gurr, E. *Staining-Practical and Theoretical*, 2nd ed.; Williams and Watkins: Baltimore, Md. 1962; p 303.

(10) Lamanna, J. C.; Mc Cracken, K. A. *Anal. Biochem*. **1984**, *142*, 117−125.

(11) Singh, M. K.; Pal, H.; Bhasikuttan, A. C.; Sapre, A. V. *Photochem. Photobiol*. **1999**, *69*, 529−535.

(12) Singh, M. K.; Pal, H.; Bhasikuttan, A. C.; Sapre, A. V. *Photochem. Photobiol*. **1998**, *68*, 32−38.

(13) Allison, A. C.; Magnus, I. A.; Young, M. R. *Nature* **1966**, *209*, 874−878.

(14) Chen, Q. Y.; Li, D. H.; Zhao, Y.; Yang, H. H.; Zhu, Q. Z.; Xu, J. G. *Analyst* **1999**, *124*, 901−906.

(15) Shimamori, H.; Hanamuro, K.; Tatsumi, Y. *J. Phys. Chem*. **1993**, *97*, 3545−3550.

(16) John Plater, M. *Arkivoc* **2003**, (*i*), 37−42.

(17) Becke, A. D. *J. Chem. Phys*. **1993**, *98*, 5648−5652.

(18) Frisch, M. J.; Trucks, G. W.; Schlegel, H. B.; Scuseria, G. E.; Robb, M. A.; Cheeseman, J. R.; Montgomery, J. A.; Vreven, T., Jr.; Kudin, K. N.; Burant, J. C.; Millam, J. M.; Iyengar, S. S.; Tomasi, J.; Barone, V.; Mennucci, B.; Cossi, M.; Scalmani, G.; Rega, N.; Petersson, G. A.; Nakatsuji, H.; Hada, M.; Ehara, M.; Toyota, K.; Fukuda, R.; Hasegawa, J.; Ishida, M.; Nakajima, T.; Honda, Y.; Kitao, O.; Nakai, H.; Klene, M.; Li, X.; Knox, J. E.; Hratchian, H. P.; Cross, J. B.; Adamo, C.; Jaramillo, J.; Gomperts, R.; Stratmann, R. E.; Yazyev, O.; Austin, A. J.; Cammi, R.; Pomelli, C.; Ochterski, J. W.; Ayala, P. Y.; Morokuma, K.; Voth, G. A.; Salvador, P.; Dannenberg, J. J.; Zakrzewski, V. G.; Dapprich, S.; Daniels, A. D.; Strain, M. C.; Farkas, O.; Malick, D. K.; Rabuck, A. D.; Raghavachari, K.; Foresman, J. B.; Ortiz, J. V.; Cui, Q.; Baboul, A. G.; Clifford, S.; Cioslowski, J.; Stefanov, B. B.; Liu, G.; Liashenko, A.; Piskorz, P.; Komaromi, I.; Martin, R. L.; Fox, D. J.; Keith, T.; Al-Laham, M. A.; Peng, C. Y.; Nanayakkara, A.; Challacombe, M.; Gill, P. M. W.; Johnson, B.; Chen, W.; Wong, M. W.; Gonzalez, C.; Pople, J. A. *Gaussian 03*, revision B.05; Gaussian Inc., Pittsburgh PA, 2003.